RSC Advances

ROYAL SOCIETY OF CHEMISTRY

www.rsc.org/advances

Cite this: DOI: 10.1039/c0xx00000x

www.rsc.org/xxxxxx

ARTICLE TYPE

Photothermal healing of glass fiber reinforced composites interface by gold nanoparticles

Zhenxing Cao[a], Rongguo Wang[a]*, Fan Yang [a], Lifeng Hao[a]*, Weicheng Jiao[a], Wenbo Liu[b], Qi Wang[a] and Boyu Zhang[a]

Received (in XXX, XXX) Xth XXXXXXXXX 20XX, Accepted Xth XXXXXXXXX 20XX
DOI: 10.1039/b000000x

Formation of microcracks especially in the interfacial region is a critical problem for fiber reinforced composites. Repairing the microcracks before catastrophic failure of the materials taking place is a promising solution to achieve long lifetime operation. In this context, a novel method is demonstrated for interfacial healing of glass fiber reinforced composites using photothermal effect of gold nanoparticles (Au NPs). Au NPs were successfully dispersed into the interfacial region of glass fiber reinforced composite. Once the interfacial damage occurred, a laser could be used to illuminate Au NPs to generate a large amount of heat through the photothermal effect. This would melt the resin and form mechanical interlock between the fiber and PMMA to create a new interface. It has been confirmed by micro bond test that the composite containing Au NPs has the healing ability with a maximum healing efficiency of 98.5 % under optimized conditions. The mechanism of the interfacial healing was also investigated and it is found that the density of Au NPs and irradiation intensity play the key roles in the healing process.

Introduction

The photothermal effect of gold nanoparticles (Au NPs) refers to surface plasmon resonance mediated heating, wherein incident light energy is converted into heat[1]. The temperature near a single Au NP can be quickly raised for more than thousands degrees making the effect an interesting and versatile tool for localized heating in nanoscale. Many applications have been reported, such as targeted drug delivery[2, 3], cancer therapy[4-8] or chemical deposition[9, 10]. Recently, this technique has been applied to thermal manipulation of polymers. For instance, Alessandri et al. exploited plasmonic heating to "write" with a laser by ablating a polymeric surface coated with gold nanoparticles[11]. Maity et al. discussed an alternative approach for selectively thermal treatment of polymeric materials[12, 13]. Haas et al. reported the thermal degradation of a solid film of polypropylene carbonate, driven by the photothermal effect of Au NPs[14]. Hongji Zhang et al. demonstrated a general method for healing the strong hydrogel, shape memory polymer and crystalline polymer using this method[15-17].

As a novel but efficient heating method for polymer materials, the photothermal effect can be easily implemented to polymer based composites, particularly for handling the regions which are vulnerable to the attack of micro cracks but not easy to be repaired by conventional heating methods. A good example is the interface between fiber and matrix, which acts as an intermediate bridge and transfers the load from matrix to fiber through the shear flow. It is extremely importance to the mechanical and physical behavior of the composite[18], but it is also susceptible to failure. Once the interface debonded, the damage tends to propagate along the interface after repeated loading, develops into large-scale damage and ultimately leads to failure of the whole composite. Therefore, it is necessary to heal the interface avoiding crack propagation. But there are only a few of interfacial healing schemes have been reported in the literature[19-24], because of the facts that the interface is buried inside polymer and its region has limited dimensions (approximately 200-300nm on top of glass fibers).

In this work, we presented a method for local interfacial healing of glass fiber reinforced thermoplastic composite via local heating ability of Au NPs. For interfacial healing, glass fibers were functionalized by coating Au NPs through chemical self-assembled[25, 26], which were used to prepare micro bond test samples. The interfaces of these samples were debonded by micro bond test and then healed under laser irradiation. The healing ability and mechanism were investigated. Experimental results show that the composite functionalized with Au NPs has the capability to heal interface and the optimum healing efficiency could be obtained through controlling the density of Au NPs and irradiation intensity.

Experimental

Materials

The chlorauric acid ($HAuCl_4 \cdot 4H_2O$), aqueous trisodium citrate

[a] Center for Composite Materials and Structures, Harbin Institute of Technology, Harbin, 150080, China. E-mail: wrg@hit.edu.cn, hlf@hit.edu.cn
[b] School of Materials Science and Engineering, Harbin Institute of Technology, Harbin, 150001, China.

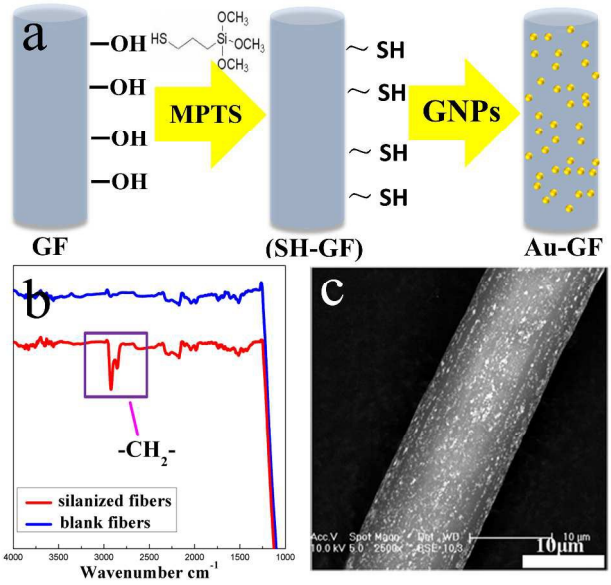

Fig. 1. (a) The process to prepare functional glass fiber, (b) FTIR spectra of the samples and (c) SEM image of Au NPs coated glass fiber modified by 30 g/L MPTS.

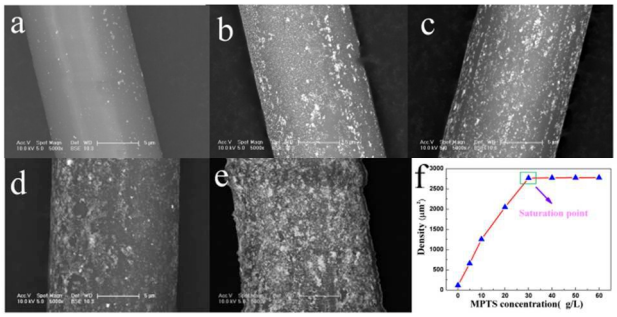

Fig. 2. SEM images of Au NPs coated fibers modified by MPTS with different concentration (a: 0 g/L, b: 5 g/L, c: 10 g/L, d: 20 g/L and e: 30 g/L). (f) Coating density of Au NPs on the fiber surface as a function of MPTS concentration.

($Na_3C_6H_5O_7 \cdot 2H_2O$), polyvinylpyrrolidone (PVP) and 3-mercaptopropyl trimethoxysilane (MPTS) were purchased from J&K Chemical Ltd. Commercially available glass fiber was purchased from JUSHI, China. The polymethyl methacrylate (PMMA) was provided by Wuxi Resin Factory, China and its glass transition temperature (T_g) is 120 ℃. The chloroform, acetone, hexane and ethanol were provided by Aladdin, which are high performance liquid chromatographic grade.

Preparation of micro bond test samples

The glass fiber was heated at 500 ℃ for 2 h to remove the surfactant. Then it was sequentially cleaned by ultrasonic in acetone for 15 min and in ethanol for 15 min, and was dried at 80 ℃ for 1 h. The pretreated glass fiber was functionalized by MPTS solutions with different concentration in hexane at room temperature for 30 min and the pH was controlled at 4 by using HCl. After being isolated from the silane solution, the glass fiber was heated at 120 ℃ for 1 h to form a silica treated layer. Afterward the silanized fiber was immerged in a 100 mL Au NPs bath synthesized by the Frens method[27] for self-assembly for 30 min. Then the Au NPs coated glass fiber was carefully rinsed with deionized water in ultrasonic assisted environment and dried in an oven at 110 ℃ for 2 h. Finally some PMMA micro-droplets with length of 40–120 μm were adhered on the Au NPs coated fiber filament to form samples used in micro bond test. The prepared samples were shaped in an air dry oven under the normal pressure at 150 ℃ for 30 min.

Healing procedure

Interfacial debonding was induced by micro bond test. After debonding, the deformed sample was irradiated with a 532 nm continuous wave diode laser with the power of 150 mw for 5 min to excite the photothermal effect of Au NPs. The beam size of the laser could be continuously adjusted from 3 mm to 100 μm via lens. To determine the healing efficiency accurately, debonding and healing were repeatedly applied to more than twenty samples. The healing efficiency is defined as

$$\eta = \frac{\tau_{\text{Healed}}}{\tau_{\text{Virgin}}} \quad (1)$$

where η is the healing efficiency, τ_{healed} is the interfacial shear strength (IFSS) of healed sample and τ_{virgin} is the IFSS of virgin sample.

Characterizations

Extinction spectra of Au NPs solution diluted with water was measured with a ultra-violet visible spectrometer (Cary 5000, Agilent) to identify the location of the surface plasmon resonance. The observation of Au NPs was performed with a transmission electron microscopy (JEM 2100F, JEOL LTD) under an acceleration voltage of 200 KV. FTIR spectra of glass fiber was studied by Fourier transform infrared spectrophotometer (BX-II, Perkin Elmer).The micrographs of the fiber coated with Au NPs were taken by using field emission scanning electron microscope (JSF 6700F, JEOL LTD) with energy-dispersion X-ray analysis (EDX). A power meter (TPM 300CE, Gentec Electro Optics) was used to measure and verify the power of the laser. IFSS was tested using micro bond methods in interface strength tester (MODEL HM410, TOHEI SANGYO). The IFSS (τ) is calculated according to the Eq. 2,

$$\tau = \frac{F_{\max}}{\pi d l} \quad (2)$$

where F_{max} is the maximum force, d is the corresponding fiber diameter and l is the embedded length.

Results and discussion

Functionalization of fiber glass interface

The fibers with interfacial healing ability were prepared by coating fibers with Au NPs using chemical self-assembly. Silanes act as a bridge to connect the fiber and Au NPs together. As manifested in Fig. 1a, the methoxy groups (OCH_3) of the silane coupling agent MPTS hydrolyzed in the presence of water and formed silanols. The silanols are then expected to react with the naturally occurring hydroxyl group on the glass fiber surface and form siloxane linkages or with each other to form a polysiloxane coating on the glass fiber surface[28]. This process makes the MPTS –SH groups anchored on the glass fiber surface. Then

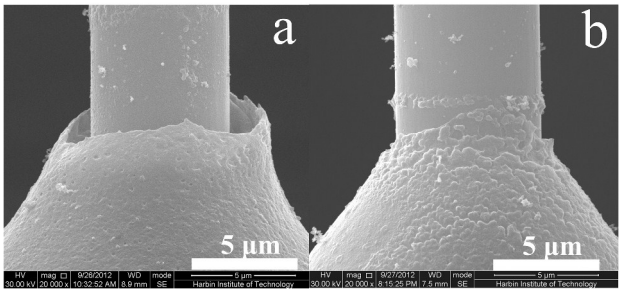

Fig. 3. The SEM images of debonded sample before healing (a) and after healed (b).

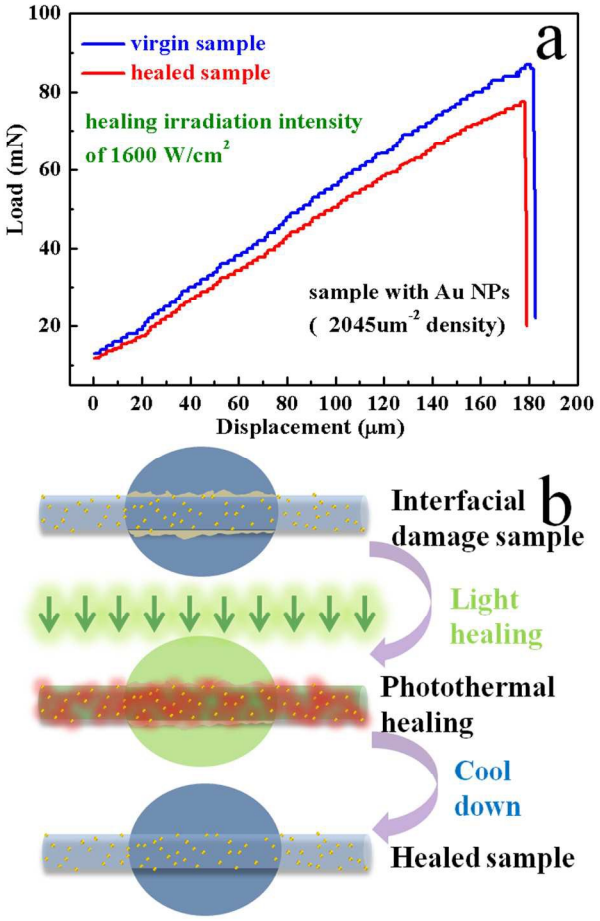

Fig. 4. (a) Typical load displacement curves of virgin (blue) and healed (red) sample with Au NPs for microbond testing and (b) Scheme of interfacial healing process.

gold-thiolate bonds are formed between the Au NPs and –SH[29, 30], which leads to Au NPs layer firmly attach to the silanized glass fiber. The reaction between silanes and fiber is confirmed by FTIR spectra in Fig. 1b. Significant change is observed in the spectra of silanized fibers. The bands where the stretching vibration of $–CH_2–$ take place at 2853 and 2931 cm^{-1} confirming that MPTS with –SH is obtained on pretreatment glass fiber. And the SEM image in Fig. 1c shows high yield Au NPs uniformly distributed on the fiber surface, which indicates the success of chemical self-assembly.

A series of fibers with different coating density could be obtained by changing the concentration of MPTS solution while keeping other parameters constant. Fig. 2(a-e) show the SEM images of fiber surfaces modified by MPTS with different concentration (0, 5, 10, 20 and 30 g/L). It is note that, without MPTS, only a small amount of Au NPs scattered on the fiber surface as shown in Fig. 2a. With MPTS, a significant increase of the coating density can be observed as shown in Fig. 2(b-e), mainly due to the concentration of MPTS solution controls the silanized degree of glass fiber and affects the affinity of the Au NPs to the fiber surface. The coating density increases linearly with MPTS concentration, as shown in Fig.2 (f), and saturated at 2766 μm^{-2} for a concentration of 30 g/L.

Interfacial healing by photothermal effect

The interfacial healing process is carried out on the micro bond test machine on which the interface debonding can be created in a controlled manner and the IFSS can be measured quantitatively. The Fig. 3 shows the SEM images of a resin droplet before and after healing. There is apparent debonding between the fiber and PMMA resin before healing. We can see the fiber exposure at the debonding position. After irradiating healing 5 min with a laser of 1600 W/cm^2, the morphology of the deformed sample is significantly modified at the debonding position and it is clear that the exposed fiber was recovered by PMMA. There is a new interface formed by the mechanical interlock between the fiber and PMMA. At the same time, the displacement curves are shown in Fig. 4a for the virgin and healed samples with coating density of 2045 μm^{-2}. The sample was loaded continuously until full interfacial debonding occurs at about 87mN. Then after 5 min laser illuminating with irradiation intensity of 1600 W cm^{-2}, the sample was re-tested and the debonding load was 77 mN, corresponding to a healing efficiency of 88.5%.

This healing behavior is due to the special local heating of Au NPs and the envisioned healing process is schematically illustrated in Fig. 4b. Firstly, the interfacial damage was induced by the micro bond test. Then the 532nm laser applied to the interfacial region, which strongly drives mobile carriers inside the Au NPs and the energy gained by these carriers is turned into heat[1, 31]. The heat then diffuses away from the Au NPs leading to an elevated temperature above the T_g of the PMMA resin. So that the crystallites are melted and polymer chains in the melt can diffuse across the interface. The high temperature at the interface not only melts the surrounding PMMA resin, but also forces the melt resin to diffuse inward and re-entangled to infiltrate the fiber since the thermal expansion at the interface due to the local heating was blocked by the surrounding cold matrix. After turning off the light, interdiffused polymer chains in the interfacial area are cooled resulting in immediate recrystallization, which generate mechanical interlock between the fiber and PMMA. As a result, the interface damage is healed and IFSS is recovered.

To confirm that the interfacial healing is caused by the photothermal effect, other factors should be ruled out, such as laser heating. Herein, the same healing experiment was performed on the sample without Au NPs coated. Fig. 5 shows the load−displacement curves of virgin (blue) and healed (red) sample without Au NPs. The debonding load for the healed sample is only 25 mN, much smaller than that of the virgin sample. It indicates that the thermal phase transition for the

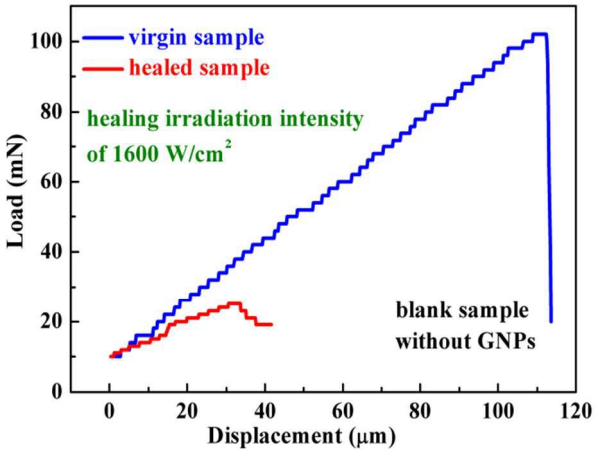

Fig. 5. Typical load displacement curves of virgin (blue) and healed (red) sample without Au NPs for microbond testing.

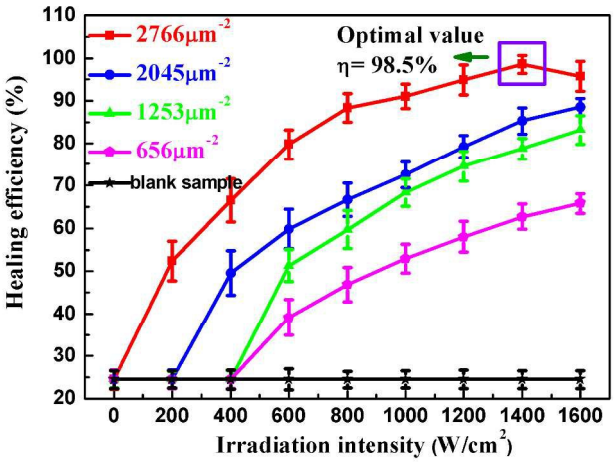

Fig. 6. Healing efficiency attained as a function of irradiation intensity for samples with different coating density

interfacial healing cannot be activated through laser irradiation without Au NPs. And the interfacial healing process relies solely on the rise of temperature generated by the local photothermal effect of the Au NPs.

Mechanism analysis of interfacial healing

In order to figure out the influence factors of the healing method and to get the optimized healing condition, it is necessary to discuss the healing mechanism further. In our experiment, the healing process is that the thermoplastic is heated by Au NPs via photothermal effect to form physical bonding and micromechanical interlocking. The process is similar to the formation of fiber reinforced thermoplastic composite, since both of them are undergone elevated temperature and then cooled. So we analyze the interfacial healing mechanism by the model, which is used to evaluate the IFSS of thermoplastic composites[32, 33]. This model assumes that in most cases, the thermal expansion coefficients of matrix polymers are much greater than that of the fibers, the cooling process results in a build-up of compressive radial stress at the interface. Assuming that the coefficient of static friction at the interface is non-zero, these compressive stresses will contribute a frictional component to the apparent IFSS. In the case of thermoplastic polymer matrices where there may often be little or no chemical bonding across the interface these static frictional stresses can make up a large fraction of the apparent IFSS. So the IFSS could be calculated theoretically as

$$\tau = \tau_0 + \mu \frac{\Delta\alpha \Delta T E_f E_m}{(1+\nu_f+2V_f)E_f + (1+\nu_m)E_m}, \quad (3)$$

where τ_0 is physiochemical molecular interactions at the interface, μ is coefficient of static friction, $\Delta\alpha$ is the difference value for thermal expansion coefficient of PMMA matrix and glass fiber, ΔT is the elevated temperature, E_f and E_m are the modulus of glass fiber and PMMA resin, ν_f and ν_m are the Poisson ratio of glass fiber and PMMA resin and V_f is the fiber volume fraction. Since μ, $\Delta\alpha$, E_f, E_m, ν_f, ν_m and V_f are constant in our experiment, for the sake of simplicity, we define

$$\beta = \mu \frac{\Delta\alpha E_f E_m}{(1+\nu_f+2V_f)E_f + (1+\nu_m)E_m}. \quad (4)$$

Thus Eq.3 could be rewrited as

$$\tau = \tau_0 + \beta\Delta T. \quad (5)$$

In our experiment, the ΔT is determined by the photothermal effect of Au NPs, which could be calculated theoretically as[34, 35]

$$\Delta T = \frac{R_{NP}^3}{3k_0}\frac{\omega}{8\pi}\left|\frac{3\varepsilon_0}{2\varepsilon_0+\varepsilon_{NP}}\right|^2 \mathrm{Im}\,\varepsilon_{NP}\frac{8\pi}{c\sqrt{\varepsilon_0}}N_{NP}I_0, \quad (6)$$

where R_{NP} is the radius of Au NP, k_0 is the thermal conductivity of the surrounding medium, ω is the angular frequency of the light wave, ε_{NP} and ε_0 are the dielectric constants of the Au NP and surrounding medium respectively, N_{NP} is the density of Au NPs, I_0 is the light intensity inside the matrix. In this experiment, R_{NP}, k_0, ω, ε_{NP} and ε_0 are constant, therefore, we define

$$\phi = \frac{R_{NP}^3}{3k_0}\frac{\omega}{8\pi}\left|\frac{3\varepsilon_0}{2\varepsilon_0+\varepsilon_{NP}}\right|^2 \mathrm{Im}\,\varepsilon_{NP}\frac{8\pi}{c\sqrt{\varepsilon_0}}. \quad (7)$$

So ΔT can be expressed as

$$\Delta T = \phi N_{NP} I_0 \quad (8)$$

The interfacial healing in our experiment is basically a phase transition process. Thus, the healing process cannot be initialized until ΔT is above the T_g. So combining Eq. 1, 5 and 8, the healing efficiency can be calculated by Eq. 9,

$$\eta = \tau_0/\tau_{\text{virgin}} \qquad (\Delta T < T_m)$$
$$\eta = \tau_0/\tau_{\text{virgin}} + \beta\phi N_{NP} I_0/\tau_{\text{virgin}} \qquad (\Delta T \geq T_m) \quad (9)$$

Eq. 9 shows that the healing efficiency is determined by both Au NPs density and irradiation intensity under the aforementioned experimental conditions. To verify it, we investigated the effects of different Au NPs density and irradiation intensity on the healing efficiency. Fig. 6 shows the healing efficiency as a function of irradiation intensity for samples with different coating density, in which we note several interesting results. Firstly, for

blank sample, the healing efficiency is very small and independent of the irradiation intensity, as expected. On the contrary, all the Au NP coated samples recovered the IFSS under illumination. A threshold is observed, which corresponds to the melting temperatures, in accord with Eq. 9. It is easy to understand that the interfacial healing could not trigger until the irradiation intensity reaches a certain threshold. And the high temperature is obtained more easily for sample with higher coating density, so its threshold is smaller. It is also found that, as the irradiation intensity increased, the healing efficiency increases at a roughly linear rate for irradiation intensity in agreement with Eq.8. At the same time, the sample with higher density always obtained higher healing efficiency. These healing behaviours are basically consistent with our expectations, though some deviations exist. Firstly, the healing efficiency is not precisely linear increase with irradiation intensity and coating density. This could be ascribed to the non-ideal effects in the experiments, such as the heat dissipation to the surrounding, interaction between Au NPs and irregular distribution of Au NPs. In addition, the healing efficiency declines for the saturated sample when the irradiation intensity over 1400 W cm^{-2}. This might be attributed to the overheating, that is, the temperature, generated by Au NPs under high irradiation intensity, is high enough to degrade the resin thermally. From the results mentioned above, we figure out that irradiation intensity and Au NPs density are important factors to the healing efficiency and the optimized healing efficiency is 98.5% achieved for the saturated samples under irradiation intensity of 1400 W cm^{-2}.

Conclusions

In conclusion, we have demonstrated a facile and accurate method for the interfacial healing based on photothermal effect of Au NPs. In the experiment, the Au NPs were coated on fiber surface using self assembly method which made the interface with the healing ability. The results showed that we got wonderful interfacial healing with the coated fiber. We also investigated the healing mechanism of this method and found that Au NPs density and irradiation intensity play the key role on the healing efficiency and a maximum healing efficiency 98.5 % is obtained under optimized condition. The work shows that Au NP with the plasmon resonances as localized sources of heat causing interfacial healing. Although we have demonstrated interfacial healing only for glass fiber reinforced PMMA composite, the principles are general and should enable to apply to most thermoplastic composite materials. The advantage of the method lies in that fact that only small amount of NP is needed to be incorporated into the parts which are most venerable to damage and under laser illumination, the healing process can be confined locally causing minimized influence to the whole structure and allowing in situ healing and repairing.

Acknowledgements

The works were financially supported by the fund of the Project supported by the National Natural Science Foundation of China (No.51303039)， National Basic Research Program of China (No.2011CB605605), Natural Science Foundation of China (No.51402067) and the Doctoral Scientific Fund Project of the Ministry of Education of China (No. 20122302120034).

Notes and references

1. S. Link and M. A. El-Sayed, Int Rev Phys Chem, 2000, 19, 409-453.
2. H. Y. Liu, T. L. Liu, X. L. Wu, L. L. Li, L. F. Tan, D. Chen and F. Q. Tang, Adv Mater, 2012, 24, 755-+.
3. D. Pissuwan, T. Niidome and M. B. Cortie, J Control Release, 2011, 149, 65-71.
4. P. K. Jain, I. H. El-Sayed and M. A. El-Sayed, Nano Today, 2007, 2, 18-29.
5. H. C. Huang, K. Rege and J. J. Heys, Acs Nano, 2010, 4, 2892-2900.
6. Y. L. Luo, Y. S. Shiao and Y. F. Huang, Acs Nano, 2011, 5, 7796-7804.
7. S. T. Wang, K. J. Chen, T. H. Wu, H. Wang, W. Y. Lin, M. Ohashi, P. Y. Chiou and H. R. Tseng, Angew Chem Int Edit, 2010, 49, 3777-3781.
8. X. C. Wang, G. H. Li, Y. Ding and S. Q. Sun, Rsc Adv, 2014, 4, 30375-30383.
9. D. A. Boyd, L. Greengard, M. Brongersma, M. Y. El-Naggar and D. G. Goodwin, Nano Lett, 2006, 6, 2592-2597.
10. W. H. Hung, I. K. Hsu, A. Bushmaker, R. Kumar, J. Theiss and S. B. Cronin, Nano Lett, 2008, 8, 3278-3282.
11. I. Alessandri and L. E. Depero, Nanotechnology, 2008, 19.
12. S. Maity, L. N. Downen, J. R. Bochinski and L. I. Clarke, Polymer, 2011, 52, 1674-1685.
13. S. Maity, J. R. Bochinski and L. I. Clarke, Adv Funct Mater, 2012, 22, 5259-5270.
14. K. M. Haas and B. J. Lear, Nanoscale, 2013, 5, 5247-5251.
15. H. J. Zhang, D. Fortin, H. S. Xia and Y. Zhao, Macromol Rapid Comm, 2013, 34, 1742-1746.
16. H. J. Zhang, D. H. Han, Q. Yan, D. Fortin, H. S. Xia and Y. Zhao, J Mater Chem A, 2014, 2, 13373-13379.
17. H. J. Zhang and Y. Zhao, Acs Appl Mater Inter, 2013, 5, 13069-13075.
18. W. J. Cantwell and J. Morton, J Strain Anal Eng, 1992, 27, 29-42.
19. B. J. Blaiszik, M. Baginska, S. R. White and N. R. Sottos, Adv Funct Mater, 2010, 20, 3547-3554.
20. A. R. Jones, B. J. Blaiszik, S. R. White and N. R. Sottos, Compos Sci Technol, 2013, 79, 1-7.
21. A. R. Jones, A. Cintora, S. R. White and N. R. Sottos, Acs Appl Mater Inter, 2014, 6, 6033-6039.
22. A. M. Peterson, R. E. Jensen and G. R. Palmese, Compos Sci Technol, 2011, 71, 586-592.
23. A. M. Peterson, R. E. Jensen and G. R. Palmese, Acs Appl Mater Inter, 2013, 5, 815-821.
24. Z. X. Cao, R. G. Wang and L. F. Hao, Rsc Adv, 2015, 5, 5680-5685.
25. A. Orza, L. Olenic, S. Pruneanu, F. Pogacean and A. S. Biris, Chem Phys, 2010, 373, 295-299.
26. B. S. Flavel, M. R. Nussio, J. S. Quinton and J. G. Shapter, J Nanopart Res, 2009, 11, 2013-2022.
27. G. Frens, K. Z., J. Turkevich, J. Hillier and P. C. Stevenson, nature physical science, 1973, 241, 20-22
28. H. Y. Cui and M. R. Kessler, Compos Sci Technol, 2012, 72, 1264-1272.
29. J. C. Love, L. A. Estroff, J. K. Kriebel, R. G. Nuzzo and G. M. Whitesides, Chem Rev, 2005, 105, 1103-1169.
30. S. Kera, H. Setoyama, K. Kimura, A. Iwasaki, K. K. Okudaira, Y. Harada and N. Ueno, Surf Sci, 2001, 482, 1192-1198.
31. S. A. Maier and H. A. Atwater, J Appl Phys, 2005, 98.
32. W. B. Liu, S. Zhang, L. F. Hao, W. C. Jiao, F. Yang, X. F. Li and R. G. Wang, Polym Composite, 2013, 34, 1921-1926.
33. J. L. Thomason and L. Yang, Compos Sci Technol, 2011, 71, 1600-1605.
34. A. O. Govorov, W. Zhang, T. Skeini, H. Richardson, J. Lee and N. A. Kotov, Nanoscale Res Lett, 2006, 1, 84-90.
35. A. O. Govorov and H. H. Richardson, Nano Today, 2007, 2, 30-38.